SCIENTIFIC REPORTS

OPEN

SUBJECT AREAS:
MOLECULAR BIOLOGY
CELL GROWTH

Received
10 June 2014

Accepted
11 July 2014

Published
7 August 2014

Correspondence and requests for materials should be addressed to Z.J.Y. (yangzhijian1966@gmail.com) or Y.B.G. (ybge@njmu.edu.cn)

$p27^{kip1}$ haplo-insufficiency improves cardiac function in early-stages of myocardial infarction by protecting myocardium and increasing angiogenesis by promoting IKK activation

Ningtian Zhou[1], Yuxuan Fu[2], Yunle Wang[1], Pengsheng Chen[1], Haoyu Meng[1], Shouyu Guo[1], Min Zhang[1], Zhijian Yang[1] & Yingbin Ge[2]

[1]Department of Cardiology, The First Affiliated Hospital of Nanjing Medical University, Nanjing, People's Republic of China, [2]Department of Physiology, Nanjing Medical University, Nanjing, People's Republic of China.

$p27^{kip1}$ (p27) is widely known as a potent cell cycle inhibitor in several organs, especially in the heart. However, its role has not been fully defined during the early phase of myocardial infarction (MI). In this study, we investigated the relationships between p27, vascular endothelial growth factor/hepatocyte growth factor (VEGF/HGF) and NF-κB in post-MI cardiac function repair both in vivo and in the hypoxia/ischemia-induced rat myocardiocyte model. In vivo, haplo-insufficiency of p27 improved cardiac function, diminished the infarct zone, protected myocardiocytes and increased angiogenesis by enhancing the production of VEGF/HGF. In vitro, the presence of conditioned medium from hypoxia/ischemia-induced p27 knockdown myocardiocytes reduced the injury caused by hypoxia/ischemia in myocardiocytes, and this effect was reversed by VEGF/HGF neutralizing antibodies, consistent with the cardioprotection being due to VEGF/HGF secretion. We also observed that p27 bound to IKK and that p27 haplo-insufficiency promoted IKK/p65 activation both in vivo and in vitro, thereby inducing the NF-κB downstream regulator, VEGF/HGF. Furthermore, IKKi and IKK inhibitor negated the effect of VEGF/HGF. Therefore, we conclude that p27 haplo-insufficiency protects against heart injury by VEGF/HGF mediated cardioprotection and increased angiogenesis through promoting IKK activation.

Although the function of p27 has been extensively studied in various cancers[1,2] and in organ development[3,4], the effects of p27 on myocardial infarction (MI) remain incompletely understood. As a terminally differentiated organ, the adult mammalian heart has very limited regenerative capacity[5], and high levels of $p27^{kip1}$ (p27) have been observed in cardiomyocytes. However, the hearts of neonatal rodents and of humans of up to 7 months of age retain proliferative capacity[6]. Cardiomyocytes subsequently lose the ability to divide; they switch from hyperplastic to hypertrophic as they withdraw from the cell cycle and remain in the G0 stage of the cell cycle indefinitely[7–9]. As previously reported, p27 haplo-insufficient and deficient mice exhibit pro-angiogenesis action and overall increased growth of various organs, including heart, spleen, and liver compared with wild type (WT) mice[10,11] and possibly exhibit increased re-entry of adult cardiomyocytes into the cell cycle after injury[12,13].

The incidence of heart attacks, especially those due to myocardial infarction has rapidly increased worldwide. MI leads to a poor prognosis[14], and it is crucial to restore the ischemic area blood flow immediately and preserve the ischemic myocardium. Therapeutic angiogenesis by autocrine and paracrine signaling is widely accepted in academic fields[15], including the use of a variety of angiogenic cytokines, which play an initial role in counteracting hypoxia and ischemia and in regulating the microenvironment by increasing collateral vascular growth, promoting cardiomyocyte proliferation and limiting fibrosis in the affected area. Currently, animal and clinical data

indicate that the transfer of genes for angiogenic factors, including FGF[16–18], vascular endothelial growth factor (VEGF)[19–21], angiopoietin[21,22] and hepatocyte growth factor (HGF)[23], into the ischemic myocardium can induce pro-angiogenesis action and improve cardiac function. Interestingly, in many cancer tissues, VEGF, HGF and p27 can interact to regulate angiogenesis or lead to the redistribution of blood vessels[24–26]. Evidence shows that hypoxia and serum deprivation decrease p27 expression[27] and that low levels of p27 expression increased VEGF[26] and HGF[25] production.

Following myocardial ischemia, NF-κB is a key regulator of inflammatory and survival pathways and is activated by increased IKK activation. At the early stage of injury, including the development of ischemia and hypoxia, inflammation is an automatic trigger that counteracts negative factors and maintains biological function. NF-κB is thought to be an intracellular messenger that transmits the gene induction signal from the cytoplasm to the nucleus. Importantly, although the location of the NF-κB binding site-like element in the HGF gene is far from the major transcription initiation site, the HGF gene also is activated by the production of NF-κB, which is induced by a variety of factors, including TNF-α, IL-1 and TPA[28]. VEGF is widely known as a downstream factor in the NF-κB pathway. Huang and co-workers reported that low levels of p27 expression promote IKK/NF-κB p65 activation[29]. Among the molecular mechanisms involved, cell cycling and inflammation are of paramount importance not only for protecting the cells but also for improving angiogenesis; thus, the various effects of VEGF and HGF are important for the repair of heart injury. However, few studies have examined the relationships between p27, NF-κB, VEGF and HGF in MI.

In the present study, we examined whether p27 haplo-insufficiency affects the progression of MI in mice. After ligation of the left anterior descending (LAD) coronary artery, echocardiography was used to investigate the cardiac function of p27 haplo-insufficient and WT mice. We tested NF-κB pathway activation as well as VEGF and HGF secretion in vitro and in vivo. We verified that pro-angiogenesis activity and cardiomyocyte protection improved the prognosis in p27 haplo-insufficient post-MI mice by promoting NF-κB activation.

Results

$p27^{+/-}$ mice exhibit increased cardiac function after MI. Myocardial infarction (MI) was induced by LAD artery ligation in WT, $p27^{+/-}$ and $p27^{-/-}$ mice. Of 10 $p27^{-/-}$ mice, 8 (80%) died within 6 days of LAD artery ligation; no deaths were observed in sham, WT and $p27^{+/-}$ mice 28 days after LAD artery ligation. Thus, we chose the $p27^{+/-}$ mice, which expressed half the normal level of p27 protein in all tissues, including the heart, for subsequent experiments to determine the underlying mechanisms. At 28 days after MI, significant systolic dysfunction was observed, as assessed by the left ventricular (LV) fractional shortening (FS%) and ejection fraction (EF%) in infarcted groups compared with the controls (*$p < 0.05$, WT MI/$p27^{+/-}$ MI versus WT sham/$p27^{+/-}$ sham). However, LV dysfunction was attenuated in $p27^{+/-}$ mice compared with WT mice after infarction (#$p < 0.05$, $p27^{+/-}$ MI versus WT MI, Figure 1A). These data suggest that the haplo-insufficiency of p27 preserves cardiac function after MI.

$p27^{+/-}$ mice exhibit reduced cardiac injury and better heart formation after MI. TUNEL-positive cardiomyocytes were significantly less frequent in $p27^{+/-}$ mice than in WT mice (*$p < 0.05$, $p27^{+/-}$ MI versus WT MI). No TUNEL-positive cells were found in the sham groups (Figure 1B). Furthermore, to determine whether decreased p27 expression attenuates cardiac injury, we assessed the size of the fibrotic area using Masson trichrome staining of the WT and $p27^{+/-}$ hearts 28 days after MI. The fibrotic areas of the $p27^{+/-}$ hearts were 30%–40% of those of the WT post-MI hearts (*$p < 0.05$, $p27^{+/-}$ MI versus WT MI, Figure 1C), consistent with previous reports. Heart formation is an extremely complex process and is regulated by specific cardiac development-related transcription factors, including MEF2 and GATA4. As shown in Figure 1G and H, $p27^{+/-}$ mice exhibited significantly higher levels of MEF2c and GATA4 than WT mice after MI. Moreover, p27 expression decreased at day 3 after MI until, at day 28, the expression of p27 was beyond the base line (Figure 1D).

$p27^{+/-}$ mice exhibit enhanced cardiac angiogenesis. Angiogenesis is known to be critical in preserving cardiac function in response to ischemic stress[31]. To determine the effects of p27 haplo-insufficiency on angiogenesis after MI, we examined capillary density in the heart tissue using isolectin IB4. The capillary density in the border zone and in the remote zone of the infarcted hearts of $p27^{+/-}$ mice was significantly higher than that in WT mice after MI (#$p < 0.05$, ψ$p < 0.05$, $p27^{+/-}$ versus WT). Similar differences were observed between the two groups after the sham operations (*$p < 0.05$, $p27^{+/-}$ versus WT Figure 1E). These data suggest that angiogenesis is greater in $p27^{+/-}$ mice than in WT mice.

$p27^{+/-}$ mice exhibit enhanced VEGF and HGF expression after MI. VEGF and HGF can induce angiogenesis in the ischemic myocardium and improve cardiac function[20,32]. To assess whether insufficient levels of p27 affect VEGF and HGF production, we analyzed VEGF and HGF expression in heart tissues using western blot analysis. As shown in Figure 2A, $p27^{+/-}$ mice exhibited significantly greater expression of VEGF/HGF and phospho-KDR/phosphor-met than WT mice ($p < 0.05$, $p27^{+/-}$ versus WT). Because the effect of cytokines is associated with the activation of their receptors, we then examined the expression of phospho-KDR (the activated VEGF receptor) and phospho-Met (the activated HGF receptor) in heart tissue using immunohistochemical staining. As shown in Figure 2B, the observed phospho-KDR positive staining was limited to endothelial cells (as assessed based on their morphology) and was markedly increased in both WT and $p27^{+/-}$ hearts after MI. Moreover, the staining intensity of phospho-KDR was significantly higher in $p27^{+/-}$ hearts than in WT hearts. Phospho-Met positive cells were found only in MI cardiomyocytes (as assessed based on their morphology), and the staining intensity in $p27^{+/-}$ hearts was significantly greater than in WT hearts (Figure 2B). These results establish that reduced levels of p27 have important anti-apoptotic effects and promote angiogenesis in the infarcted heart through the up-regulation of VEGF and HGF.

Hypoxia and TNF-α up-regulate VEGF and HGF. Hypoxia and inflammation are the initial conditions resulting from MI. To determine the mechanisms underlying the roles of VEGF and HGF in cardiac repair after MI, we examined the effects of hypoxia and TNF-α (10 ng/ml for 2 h), a key cytokine associated with inflammation, on VEGF and HGF expression in the rat myocardial cell line, H9c2. Western blotting analysis demonstrated a marked increase in VEGF and HGF expression after TNF-α and hypoxia treatment ($p < 0.05$ immediately after treatment, Figure 3A). According an ELISA (Figure 3B), H9c2 cells secreted VEGF and HGF, and this secretion increased 4 and 5-fold, respectively, when the cells were cultured in hypoxic conditions (#$p < 0.05$, Hypoxia WT/Hypoxia $p27^{knockdown}$ versus NC WT/NC $p27^{knockdown}$, Figure 3B). In contrast, VEGF and HGF were expressed at significantly higher concentrations in p27 knockdown H9c2 cells than in WT cells under both normal and hypoxic conditions (*$p < 0.05$, NC $p27^{knockdown}$/Hypoxia $p27^{knockdown}$ versus NC WT/Hypoxia WT, Figure 3B). Meanwhile, the control group did not differ significantly from the WT group. These data indicated that hypoxia promotes the production of VEGF and HGF and that decreases in the level of p27 enhance this effect.

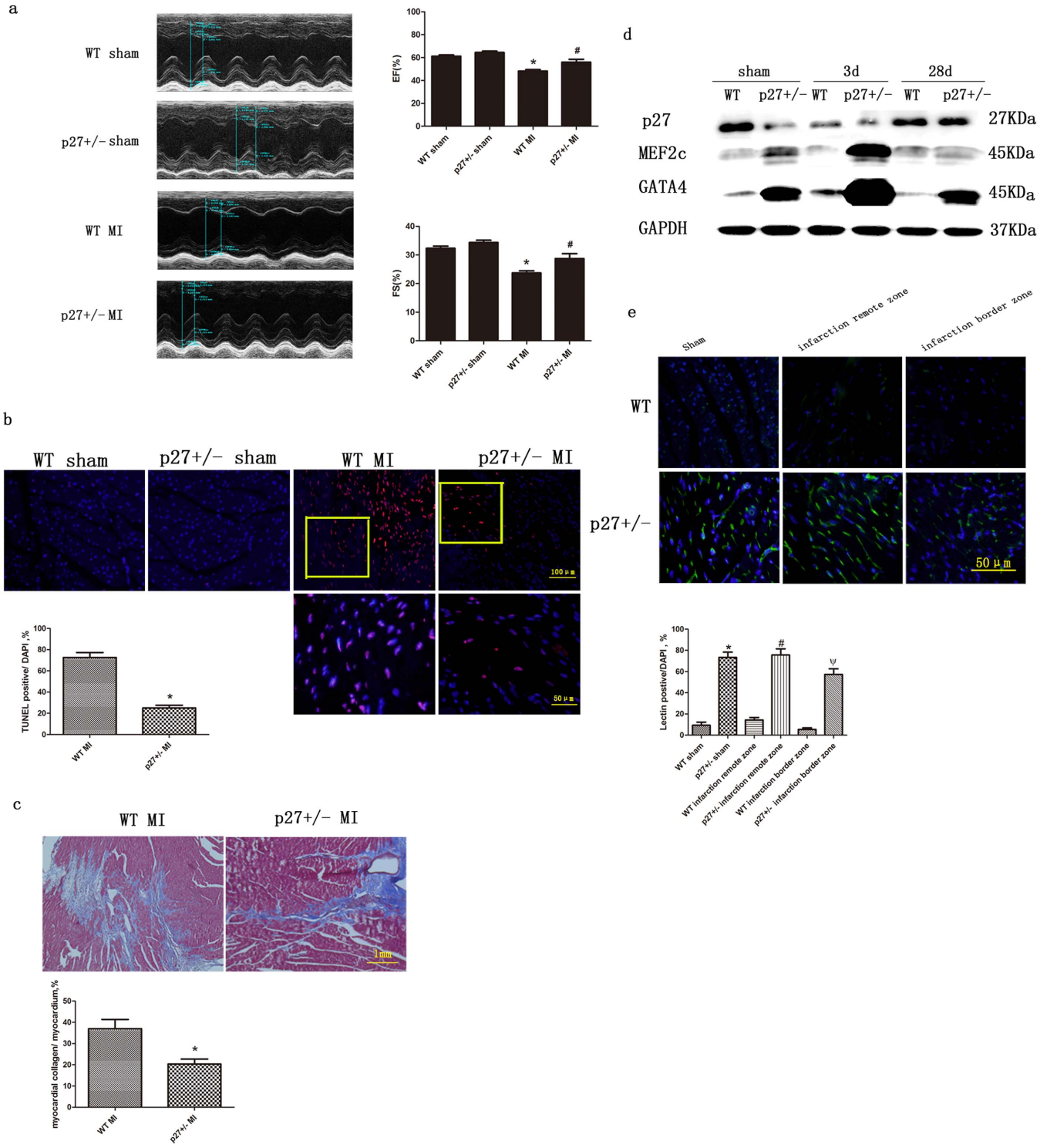

Figure 1 | The effect of p27^{kip1} haplo-insufficiency on post-infarction cardiac function, remodeling, injury and angiogenesis. (a) Representative M-mode echocardiograms from WT and p27$^{+/-}$ mice at 28 days after sham or myocardial infarction (MI) operations, groups of echocardiographic data ((n = 10 echocardiograms per echocardiographic group). *P < 0.05 versus sham; #p < 0.05 versus WT+MI. (b) Representative photomicrographs of TUNEL-positive cells (red) and nuclei (blue) in sections from sham or MI hearts. The lower panel is the enlarged box for WT+MI or p27$^{+/-}$ + MI. Quantitative analysis of TUNEL-positive cells in mouse hearts. * p < 0.05 compared with the WT + MI group. (c) Representative photomicrographs of MI hearts stained using Masson trichrome. The scar area was larger in WT mice than in p27$^{+/-}$ mice. * p < 0.05 compared with the WT MI group. (d) Representative immunoblots of MEF2c and GATA4 in the LV of p27$^{+/-}$ or WT mice at 3 and 28 days after a sham or MI operation. GAPDH served as the loading control. (e) Representative photomicrographs of IB4 lectin-positive cells (green) and nuclei (blue) in hearts after sham or MI operations. Quantitative analysis of IB4 lectin-positive cells, *p < 0.05 versus WT sham; #p < 0.05 versus WT infarction remote zone; ψp < 0.05 versus WT infarction border zone (n = 3).

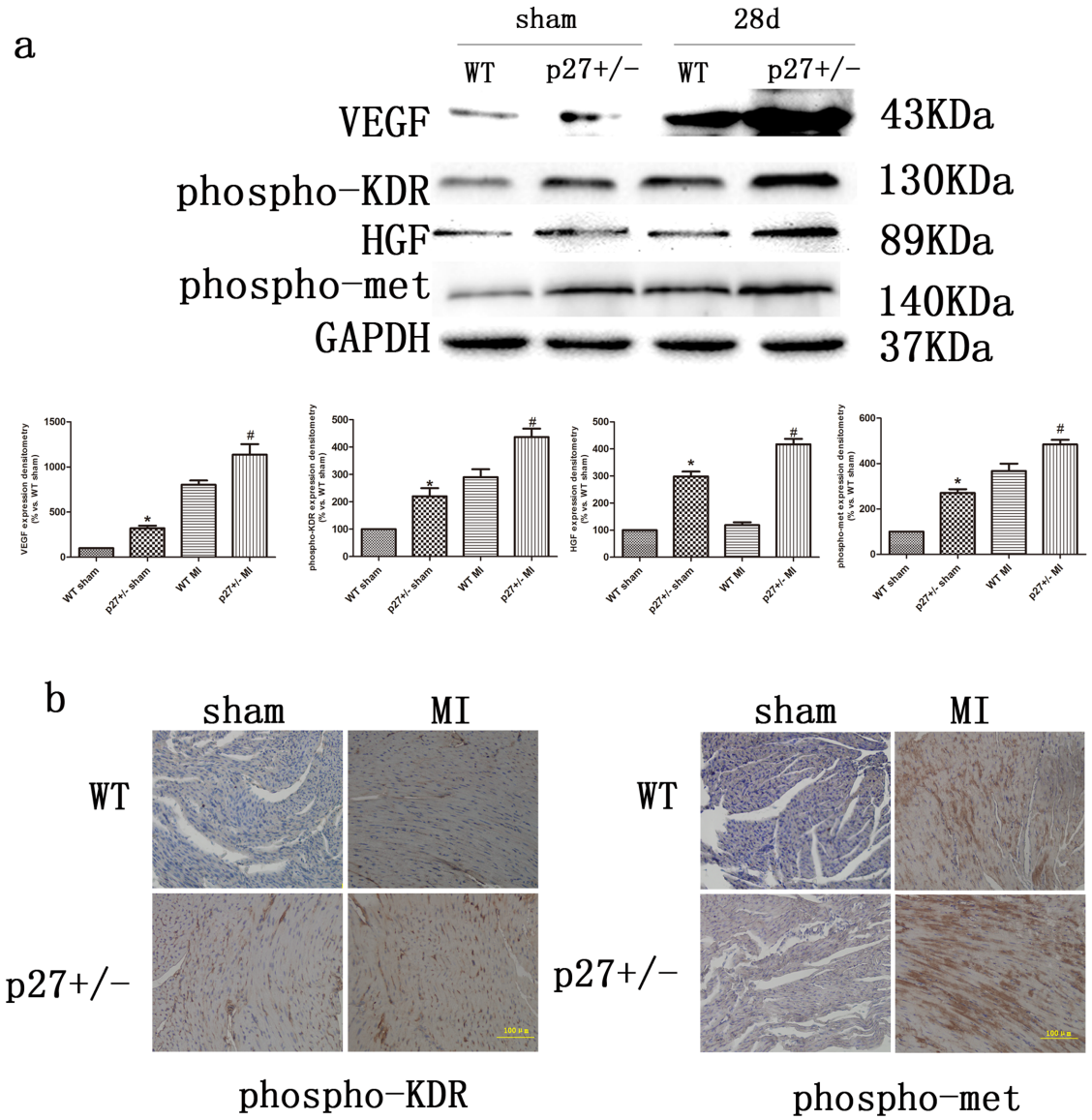

Figure 2 | The effect of p27^{kip1} haplo-insufficiency on the expression of VEGF, HGF and their activated receptors. (a) Representative immunoblots of VEGF, Phospho-KDR, HGF and phospho-Met in the LV of p27$^{+/-}$ or WT mice 28 d after treatment with sham or MI operations, according to its 43 KDa molecular weight, the up-regulated VEGF-A165 was confirmed. GAPDH served as the loading control. Quantification is shown, *$p < 0.05$ vs. WT sham; #$p < 0.05$ vs. WT MI ($n = 3$) (b) Histochemical staining of phospho-KDR in endothelial cells (upper panel) and phospho-Met in cardiomyocytes (lower panel) in mouse hearts after sham (left panel) or MI (right panel) operations.

Reduced heart injury is mediated through VEGF and HGF. To verify the cytoprotective effect of VEGF and HGF on cardiomyocytes, we measured the levels of cleaved caspase-3 and Bcl2 expression in H9c2 cells using western blot analysis. The cells were exposed to hypoxia for 12 h to mimic post-MI conditions and then treated with or without conditioned medium (CM) from hypoxia-treated p27-knockdown cells, mimicking their autocrine action. Neutralizing antibodies for VEGF and HGF were added to the CM to confirm their effects. As shown in Figure 4A, treatment with hypoxia for 12 h significant increased the levels of cleaved caspase-3 and decreased the expression of Bcl2 in H9c2 cells (12 h versus NC), indicating that hypoxia exerted a pro-apoptotic effect. These alterations in expression levels were significantly attenuated by CM treatment. Moreover, the inhibition of apoptosis by CM was partially reversed by VEGF or HGF neutralizing antibodies and was almost completely reversed when both antibodies were used in combination (CM + anti-VEGF&HGF versus CM). HGF affected the expression of phospho-Met in H9c2 cells. Thus, the cytoprotective function of CM on cardiomyocytes is mediated by VEGF and HGF.

Enhanced cardiac angiogenesis is mediated through VEGF and HGF. To verify the angiogenic effects of VEGF and HGF on the heart, we tested the effects of CM on HUVEC proliferation, migration and tube formation. HUVECs were treated with CM as previously described. As shown in Figure 4E and F, after treatment with CM, HUVEC proliferation significantly increased; HUVEC proliferation was attenuated by VEGF or HGF neutralizing antibodies and almost completely reversed when the two antibodies were used in combination. Similar results were found for the HUVEC migration and tube formation assays (*$p < 0.05$, CM/CM + HGF antibody/CM + VEGF antibody versus NC; Figure 4B, C, D). The expression of phospho-KDR and phospho-Met in HUVECs also revealed the activating effect of VEGF and HGF (Figure 4E). These results indicate that the angiogenic effects of CM are mediated by VEGF and HGF.

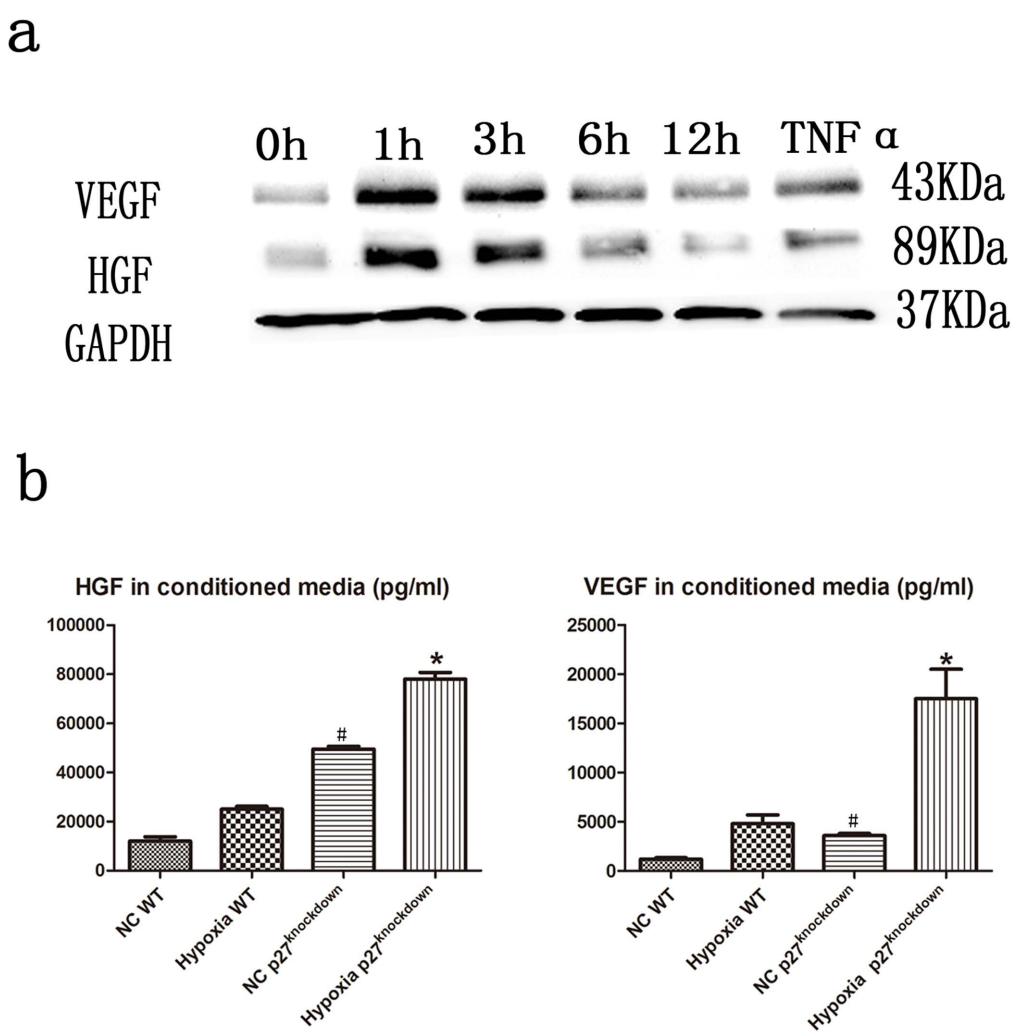

Figure 3 | VEGF and HGF expression in H9c2 cells exposed to treatment with hypoxia or TNF-α. H9c2 cells were seeded in six-well plates and then treated with hypoxia for 0, 1, 3, 6, or 12 h or with 10 ng/ml TNF-α for 2 h. (a) Representative immunoblots of VEGF and HGF in H9c2 cells treated for various times with hypoxia or with TNF-α, according to its 45 KD molecular weight, the up-regulated VEGF-A165 was confirmed. (b) VEGF and HGF levels assayed using ELISA in conditioned media. * $p < 0.05$ compared with the negative control (NC) WT group ($n = 3$).

p27 interacts with the NF-κB activator IKK. To study the p27-IKK interaction, we performed co-immunoprecipitation (Co-IP) experiments on WT mouse heart tissue lysates. As expected, binding was detected between endogenous IKKα, IKKβ and p27 in heart tissue (Figure 5A). To verify that p27 and IKK interact directly in vitro, we used a lentivirus vector to generate a stable p27 knockdown derivative of the H9c2 cell line (approximately 50% efficiency) and subjected it to hypoxia and TNF-α treatment. The phosphorylated of NF-κB activator (levels of phospho-IKKα/β) and its downstream phospho-p65 appeared to be enhanced by p27 knockdown and was associated with increased VEGF and HGF expression (*$p < 0.05$, 3 h/TNF-α versus 0 h, Figure 5B). Furthermore, we examined whether p27 affected the phosphorylation of endogenous IKK in response to MI in vivo. Indeed, IKKα and β were phosphorylated, and its downstream phospho-p65 was significantly enhanced in $p27^{+/-}$ hearts at both 3 and 28 days after MI ($p < 0.05$, $p27^{+/-}$ versus WT, Figure 5C). These data indicate that p27 interacts with IKK both in vivo and in vitro.

Enhanced expression of VEGF and HGF is mediated through p27 haplo-insufficiency and IKK α/β. To confirm the association of VEGF and HGF expression with p27 and IKKα and β, we transfected siRNA for IKKα or IKKβ into the p27-knockdown H9c2 cells and examined VEGF and HGF expression using western blot analyses. As shown in Figure 6A, the VEGF and HGF expression were both increased in cells after treatment with hypoxia for 3 h and were significantly attenuated by IKKα and IKKβ siRNAs (*$p < 0.05$, #$p < 0.05$, si-IKKα/si- IKKβ versus NC). These results were confirmed by treatment of the same cells with the IKKα/β inhibitor ACHP (*$p < 0.05$, $p27^{knockdown}$ 3 h ACHP versus $p27^{knockdown}$ 0 h; Figure 6B). These results suggest that the production of VEGF and HGF is induced by IKK activation and enhanced by p27 insufficiency.

Discussion

Damaged myocardium is replaced by fibrotic scar tissue, which compromises the contractile function of the surviving myocardium, ultimately leading to heart failure. Reactivation of the cell cycle in surviving cardiomyocytes is one strategy that can augment the number of myocytes in the diseased hearts. Potential therapeutics for MI focus on the characterization of existing models and on the combinatorial testing of various cell cycle regulators to identify the genes and/or pathways that promote cardiomyocyte proliferation. Many cell-cycle regulatory genes, including p27[32,33], have been validated by generating transgenic models with the desired gene expression patterns and evaluating their regenerative response to experimentally induced injury. Because p27 is only one component of the timing mechanism for cell cycle arrest, it cannot enable cells to exit the cell

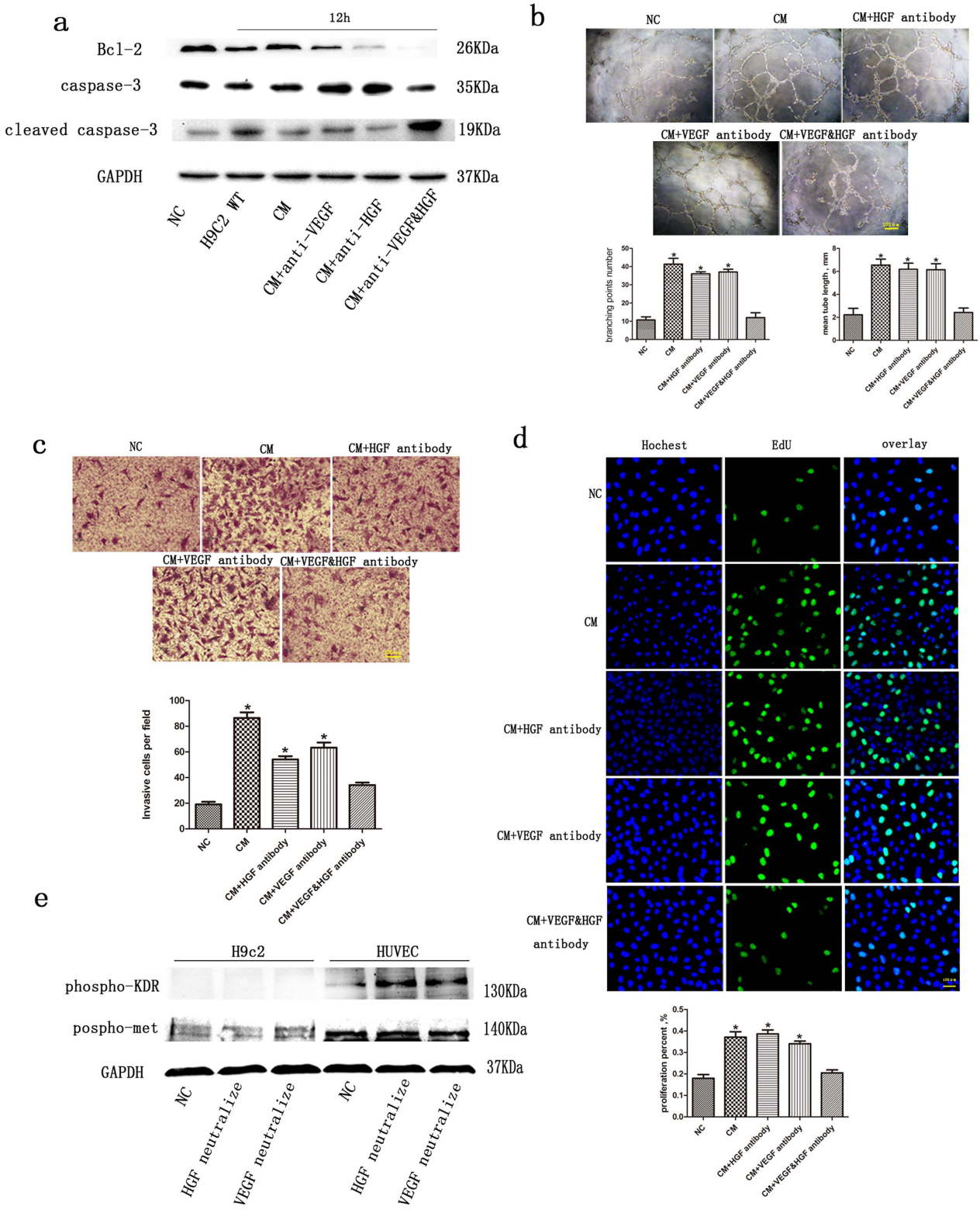

Figure 4 | Paracrine and autocrine actions of VEGF and HGF on angiogenesis and cytoprotection. (a) Representative immunoblots of Bcl-2 and cleaved caspase-3 in H9c2 cells treated with conditioned medium in the presence or absence of neutralizing antibodies after treatment with hypoxia for 12 h. GAPDH served as the loading control. The preparation of conditioned media is described in the Material and Methods section. Concentrated medium (10 μl) from $p27^{kip1}$-knockdown H9c2 cells treated with hypoxia for 12 h was applied to 1-ml cultures of HUVECs or H9c2 cells. (b) Representative photomicrographs of HUVEC tube formation assays. Quantitative analysis of tube length or branching points after various treatments. *$p < 0.05$ versus NC ($n = 3$). (c) Representative photomicrographs of HUVEC migration during transwell assays. Quantitative analysis of migrated cells after various treatments. *$p < 0.05$ versus NC. (d) Representative photomicrographs of HUVEC proliferation measured using EdU incorporation assays. The numbers of Edu positive cells after various treatments were calculated. *$p < 0.05$ versus NC. (e) Representative immunoblots of phosphor-KDR and phosphor-Met in both H9c2 cells and HUVECs treated with conditioned medium in the presence or absence of neutralizing antibodies after treatment with hypoxia for 12 h. GAPDH served as a loading control.

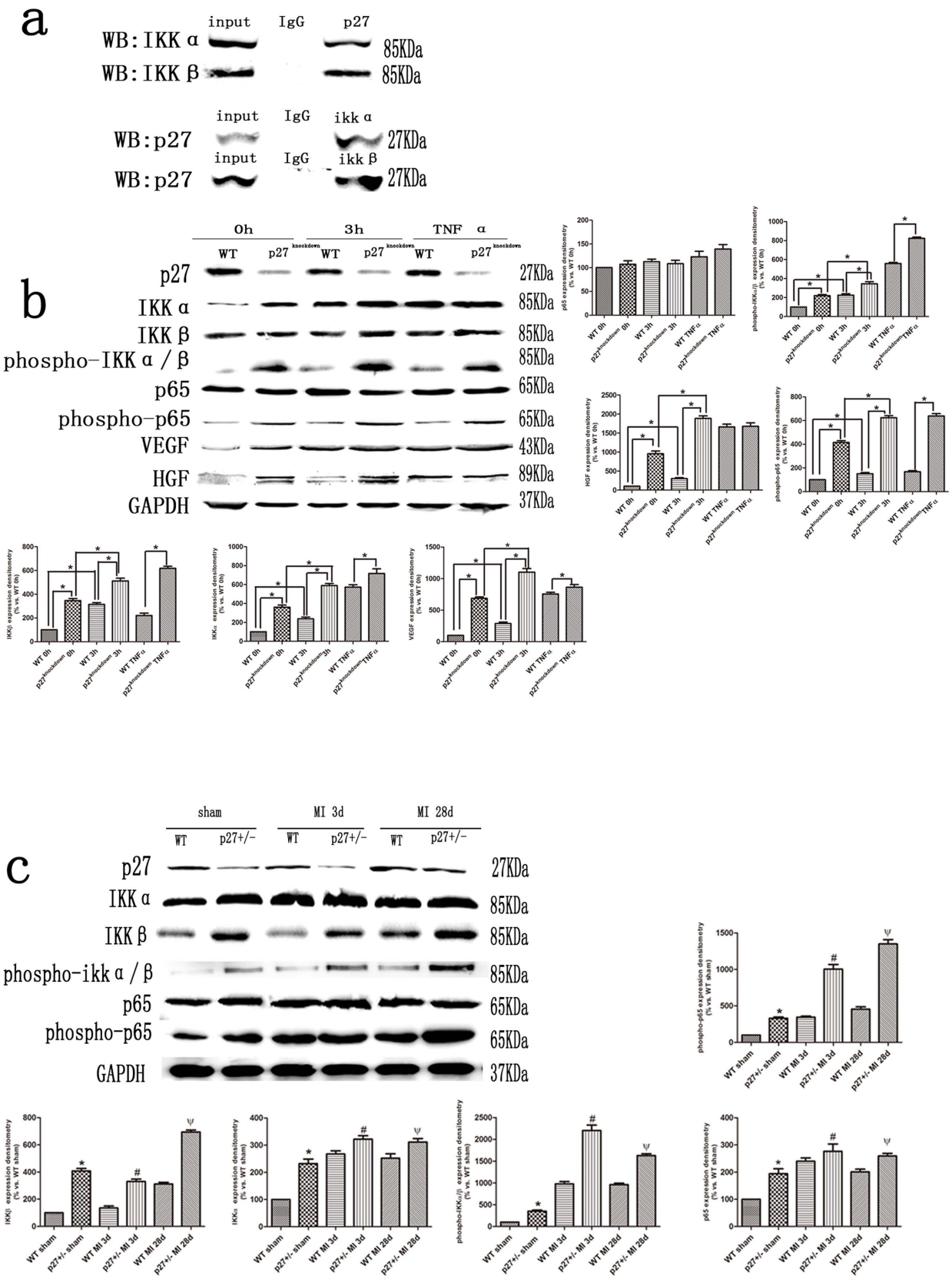

Figure 5 | p27^{kip1} interacts with the NF-κB activator, IKK. (a) Representative immunoblots of IKKα and IKKβ in heart tissue lysates precipitated using the p27^{kip1} antibody and immunoblots of p27^{kip1} in heart tissue lysates precipitated using IKKα or IKKβ antibodies. (b) Representative immunoblots of VEGF, HGF and NF-κB activation markers in p27^{kip1}-knockdown H9c2 cells exposed to treatment with hypoxia and TNF-α. GAPDH served as the loading control. Quantification is shown, *$p < 0.05$ (n = 3) (c) Representative immunoblots of NF-κB activation markers in p27$^{+/-}$ mice 3 or 28 days after MI. GAPDH served as the loading control. Quantification is shown, *$p < 0.05$ versus WT sham; #$p < 0.05$ versus WT MI 3 d; ψ$p < 0.05$ versus WT MI 28 days (n = 3).

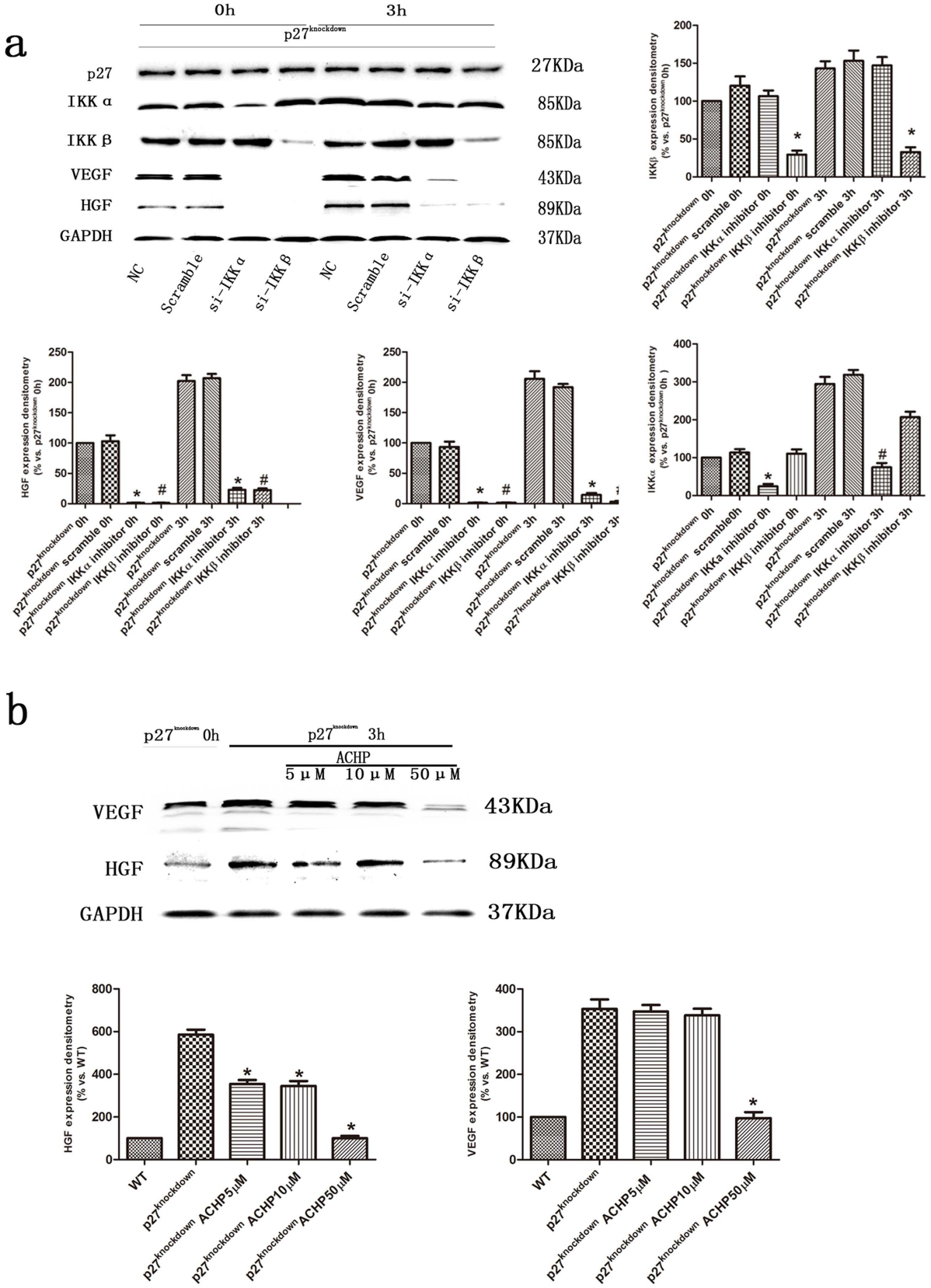

Figure 6 | The role of IKK in VEGF and HGF production in cardiomyocytes under hypoxic conditions. (a) Representative immunoblots of VEGF and HGF in $p27^{kip1}$-knockdown H9c2 cells treated with IKKα or IKKβ siRNA and then exposed to hypoxia for 3 h. GAPDH served as the loading control. Quantification is shown, *$p < 0.05$ versus p27 knockdown IKKα/IKKβ inhibitor 0 h; #$p < 0.05$ versus IKKα/IKKβ inhibitor 3 h ($n = 3$). (b) Representative immunoblots of VEGF and HGF in $p27^{kip1}$-knockdown H9c2 cells treated with the pharmacological IKK inhibitor, ACHP, and then exposed to hypoxia for 3 h. GAPDH served as the loading control. Quantification is shown, *$p < 0.05$ versus p27 knockdown ($n = 3$).

cycle by itself[33], and the partial loss of p27 might prevent cellular hypertrophy[32].

As shown in our experiments, diminished survival was found in $p27^{-/-}$ mice at the earliest stages after MI but not in WT and $p27^{+/-}$ mice. In contrast, p27 haplo-insufficient mice exhibited significant decreases in apoptosis and infarct size during early stages post MI. Improved heart function, decreased myocardium damage and increased angiogenesis were observed in $p27^{+/-}$ mice. The results revealed that p27 haplo-insufficiency plays a positive role during the early stages of post-MI repair. Moreover, following the progression of MI, p27 expression was up-regulated in both $p27^{+/-}$ and WT mice. This regulation indicates that p27 exhibits its inhibitory effect in WT and in $p27^{+/-}$ mice after the acute phase. This effect might prevent long-term ventricular decompensation remodeling and diet-induced atherosclerosis, and the partial reservation of p27 could be qualified[27,34]. Therefore, haplo-insufficiency (but not deletion) of p27 might mitigate heart injury.

Growth factors and cytokines directly activate cell growth, differentiation and survival in an autocrine- or paracrine-dependent manner in many cells. Both VEGF and HGF are crucial due to their regenerative potential; therefore, these proteins are potential candidates for therapeutic application[35–37]. Administering VEGF or HGF to cardiac cells or increasing the production of VEGF and HGF by gene transfer technology could be used to treat heart failure and improve cardiac function[38]. In this study, a significant increase in VEGF and HGF expression and their activated receptors in hearts affected by MI revealed that they play an important adaptive role after heart injury. More importantly, our results indicated that the reductions in apoptosis and infarct size and improvements in heart function and enhanced angiogenesis caused by p27 haplo-insufficiency in MI subsequently increased the production of VEGF and HGF. Similar results were observed in in vitro studies using hypoxic and ischemic cardiomyocyte models, thus suggesting the same conclusion. p27 is a potent inhibitor of cell growth and division, and p27 insufficiency might promote cell differentiation and proliferation[11,37,39]. VEGF and HGF also play an essential role in cardiac cellular reprogramming after MI[40]. Consistent with these observations, cardioprotection was enhanced in $p27^{+/-}$ mice after MI in our study, and a beneficial effect on heart injury was indicated.

The main function of p27 is to inhibit the kinase activity of cyclin dependent kinase (CDK) holoenzyme, resulting in cell-cycle arrest[41]. However, p27 also regulates motility and cell survival, suggesting that its role extends beyond cell-cycle regulation[42]. In this study, the phosphorylated of NF-κB activator was demonstrated in MI mice and enhanced by p27 haplo-insufficiency. Additionally, a p27-knockdown cardiac cell line exhibited greater sensitivity to IKK α and β phosphorylation than WT cells when subjected to both hypoxia/ischemia and TNF-α treatment (which mimic MI conditions in vivo). A co-IP experiment demonstrated that p27 could bind to the IKK α and β. Therefore, p27 knockdown might enhance the IKK α and β phosphorylation through the loss of its binding to IKK. In support of this idea, our data showed that the IKKi or IKK inhibitor ACHP reversed the increased expression of VEGF and HGF in response to hypoxia/ischemia or to TNF-α exposure.

Based on our data, we propose the following model: heart ischemic injury increases the production of VEGF and HGF, thus preventing or inhibiting the progression of heart failure through NF-κB activation. p27 haplo-insufficiency enhances VEGF and HGF expression, protecting cardiomyocytes and improving cardiac angiogenesis and cardiac function. Importantly, in the hypoxia/ischemia condition, cardiomyocytes overexpressing p27 were less viable than WT or p27-knockdown cells. This suggests that p27 does not play a repair role during early stages post MI.

Karla et al. reported that endogenous TNF-α (a potent activator of NF-κB), which is produced during the early phase of myocardial ischemia, protects cardiac myocytes against ischemic-induced apoptosis[43] and increases the expression of anti-apoptotic factors[44]. Subsequent reports have indicated that inflammation and the development of small blood vessels might limit immediate damage during a subsequent heart attack[45]. Our research provides evidence that NF-κB activation caused by p27 haplo-insufficiency might protect injured hearts during the early stages post MI. Further investigation into the physiological significance of p27 would be useful due to the potential of p27 as a target for heart failure therapy.

Methods

All reagents, siRNAs and shRNAs used in this study are described in the Supplementary Materials. All experiments were performed in accordance with relevant guidelines and regulations.

Animals. All procedures and protocols used in the present study were approved by the Nanjing Medical University Animal Care Committee and followed the guidelines of the NIH Guide for the Care and Use of Laboratory Animals. The p27-knockout ($p27^{-/-}$), p27 haplo-insufficient ($p27^{+/-}$) and strain-specific 129S4 control mice ($p27^{+/+}$, WT) were bred from a breeding pair of heterozygous p27 mice (gifts from Prof. Dengshun Miao, McGill University, Montreal, Canada) and were held in the Animal Research Center of Nanjing Medical University. The mice were bred in the SPF rodents' feeding room and maintained under appropriate conditions of temperature and humidity. Tail fragment genomic DNA was isolated using the standard phenol–chloroform extraction and isopropanol precipitation methods. The mouse genotypes were determined by PCR using tail fragment DNA as the template and the following primers: for the p27-knockout allele, the 5′ primer was CTCTCTATCGCCTTCTTG and the 3′ primer was TGGAACCCTGTGCCATCTCTAT; for the p27 wild type allele, the 5′ primer was GATGGACGCCAGACAAGC and the 3′ primer was ACGGGCTTATGATTCTGAAAGTCG. Three-month-old adult male C57BL/6 wild-type ($p27^{+/+}$), haplo-insufficient p27 ($p27^{+/-}$), and p27-knockout ($p27^{-/-}$) mice (10 per group) were randomly assigned to the MI and control groups. LAD artery ligation was used to induce MI as described. Sham animals underwent every procedure except coronary artery ligation. During the experimental trials, all mice had ad libitum access to the diet.

Cardiac Function Assessment. Experimental animals were assessed using echocardiography to evaluate cardiac function as previously described[30]. LV-end-diastolic (LVEDD) and LV-end-systolic dimensions (LVESD) were obtained using a Vevo 2100 ultrasound system (Visual Sonic Inc., Canada) equipped with a 30-MHz transducer. Fractional shortening (FS) was defined as [(LVEDD-LVESD)/LVEDD] × 100. The ejection fraction (EF) was defined as [(LVEDD3-LVESD3)/LVEDD3] × 100. For all measurements, three values were averaged for each parameter.

Histology. Heart tissues were collected from the left ventricle of mice 28 days post MI and then fixed, embedded, cut into 5-μm-thick sections and stained using HE and Masson's Trichrome.

TUNEL staining. Apoptotic nuclei were detected by in situ terminal deoxynucleotidyltransferase-mediated digoxigenin-conjugated dUTP nick-end labeling (TUNEL) using an In Situ Cell Apoptosis Detection Kit (Roche) according to the manufacturer's instructions.

Capillary density measurement. Sections were incubated with FITC-conjugated Griffonia simplicifolia lectin (Isolectin B4 1 : 20, Vector Lab, CA, USA) and mounted with Vectashield® mounting medium. Images were collected in the infarction remote zone and the infarction border zone in mice using an Olympus BX51 microscope equipped with a 10× objective. To quantify the vasculature, four independent fields (900 μm × 900 μm) were chosen randomly, and isolectin B4 positive cells were captured and analyzed using NIS Elements Basic Research Software version 2.30 (Nikon Instruments Inc., NY, USA).

Immunohistochemistry. After antigen retrieval and blocking, sections were incubated overnight at 4°C with the primary antibodies. A two-step technique was used for visualization; DAB (SK-4100 from Vector Laboratories, CA, USA) was used as the chromogen, and hematoxylin was used as the counterstain. Phosphor-KDR (#4991 1 : 200 from CST, MA, USA) and phosphor-met (#3077 1 : 200, from CST, MA, USA) were used to detect VEGF and HGF activated receptors, respectively.

Western Blot Analysis. Tissues and cells were lysed in RIPA buffer (20 mM Tris-HCl (pH 7.5), 150 mM NaCl, 1 mM Na_2EDTA, 1 mM EGTA, 1% NP-40, 1% sodium deoxycholate, 2.5 mM sodium pyrophosphate, 1 mM β-glycerophosphate, 1 mM Na_3VO_4, 1 μg/ml leupeptin). The proteins were resolved using 10% SDS-PAGE and transferred to polyvinylidene difluoride membranes (IPVH00010 from Millipore, MA, USA). After blocking, the membranes were incubated with primary antibodies and subsequently incubated with horseradish peroxidase-conjugated secondary antibodies. The resulting immunocomplexes were visualized using fluorography, as enhanced by the electrochemiluminescence system (WBKLS0100 from Millipore, MA, USA).

Immunoprecipitation. Heart tissue lysates were incubated with antibodies and protein G-agarose beads overnight at 4°C. The beads were washed and heated in 60 μl of SDS sample buffer, after which the proteins were resolved using 10% SDS-PAGE.

Cell culture and treatment. The rat myocardiac cell line H9c2 (2-1) (#GNR5, obtained from the cell bank of the Chinese Academy of Science, Shanghai, China) and human umbilical vein endothelial cells (HUVECs) (pcs-100-013, obtained from the American Type Culture Collection, MA, USA) were seeded at 1.25×10^4 cells per well in 6-well culture plates and allowed to grow for 2 days in DMEM (11995-065 from Gibco, CA, USA) containing 10% FBS (10099-141 from Gibco, CA, USA), 100 U/mL penicillin and 100 μg/mL streptomycin (450-201-EL from Winsent Inc., CA, USA). The cells were then treated as described in the figure legends. TNF-α was added to the cell culture dishes at a final concentration of 10 ng/ml for 2 hours.

Cell transfection and infection. siRNAs for IKKα, IKKβ and their scramble controls were transfected into H9c2 cells using Lipofectamine 2000 (11668-019 from Invitrogen, CA, USA). The lentivirus vector pLV-p27/kip1-inhibitor (GeneChem, Shanghai, China) and the p27overexpress plasmid (GeneChem, Shanghai, China) were used to establish stable knockdown and overexpressing cell lines from H9c2. The cells were incubated with the lentivirus vector and the plasmid in the presence of 2 μg/ml polybrene overnight and then selected using 2 μg/ml puromycin (P9620 from Sigma-Aldrich, CA, USA) to obtain stably transfected cells.

Conditioned medium preparation. H9c2 cells were washed with PBS, incubated in serum-free DMEM for 24 h and then treated with or without hypoxia in serum-free DMEM for a further 12 h. The conditioned media were collected, centrifuged at $7500 \times g$ for 20 min in 3 k centrifugal filter devices (AMICON ULTRA-4 from Millipore, MA, USA) to concentrate the samples from 10 ml to 10 μl and then stored at −80°C for further experiments.

Enzyme-linked immunosorbent assay (ELISA). HGF and VEGF levels in the media were assessed in triplicate using the Quantikine® RAT HGF and VEGF Immunoassays as described by the manufacturer. The colorimetric absorbance was determined using a microplate absorbance reader (Bio-Tek Elx800, USA), and the protein content was calculated using standard curves for recombinant HGF or VEGF.

EdU(5-ethynyl-2-deoxyuridine) incorporation assays. Incorporated EdU was detected using Click-iT® EdU Imaging Kits (C10337 from Invitrogen, CA, USA) according to the manufacturer's instructions. The cells were photographed using a fluorescent microscope (Olympus BX51 from Olympus, Tokyo, Japan), and the images were processed using Image J software (NIH). At least 50 cells were randomly selected from a single captured field. Values presented in the text are the averages calculated from five different fields.

Migration analysis. HUVEC migration was determined using a polycarbonate membrane cell culture insert (#3421 from Corning Inc., NY, USA). Cells were resuspended in DMEM containing 1% FBS in the presence or absence of conditioned media and were seeded onto the top of the wells at a density of 1×10^5 cells/well. Cells were allowed to migrate through the pores in the culture insert, which was filled with medium containing 10% FBS, for 6 h. Cells on the lower surface of the membrane were fixed and stained using Giemsa and counted and evaluated at 400-fold magnification.

Tube formation analysis. $1–2 \times 10^4$ HUVECs were seeded in 12-well plates coated with Matrigel (#356234 from BD Biosciences, NJ, USA). After 24 h, tube formation was visualized at 10× magnification using light microscopy. Tube formation was quantified by tracing along the tubes using Image J software (NIH). The number of traces per 8-bit jpeg image was quantified based on 10 different culture dishes.

Cell counting kit-8 (CCK-8) assay. Cell proliferation was measured using the cell counting kit-8 (CCK-8) assay (Dojindo, Kumamoto, Japan). Cells were seeded in triplicate in 96-well plates, and various treatments were applied. After these treatments, CCK-8 solution (10 μL) was added to each well, and the wells were incubated for a further 2 h at 37°C. The absorbance was then measured at 450 nm (Bio-Tek, Elx800, USA).

Statistical analysis. Data from at least three independent experiments were used to calculate the means ± SEM using SPSS 19.0 statistical software. Differences among the treatment groups were analyzed using Student's t-test or one-way ANOVA, followed by the Student-Newman-Keuls (SNK) test.

1. Bicknell, K. A., Coxon, C. H. & Brooks, G. Can the cardiomyocyte cell cycle be reprogrammed? *J Mol Cell Cardiol* **42**, 706–21 (2007).
2. Engel, F. B. Cardiomyocyte proliferation: a platform for mammalian cardiac repair. *Cell Cycle* **4**, 1360–3 (2005).
3. Busk, P. K. & Hinrichsen, R. Cyclin D in left ventricle hypertrophy. *Cell Cycle* **2**, 91–5 (2003).
4. Poolman, R. A. & Brooks, G. Expressions and activities of cell cycle regulatory molecules during the transition from myocyte hyperplasia to hypertrophy. *J Mol Cell Cardiol* **30**, 2121–35 (1998).
5. Murry, C. E. *et al.* Haematopoietic stem cells do not transdifferentiate into cardiac myocytes in myocardial infarcts. *Nature* **428**, 664–8 (2004).
6. Poolman, R. A., Gilchrist, R. & Brooks, G. Cell cycle profiles and expressions of p21CIP1 AND P27KIP1 during myocyte development. *Int J Cardiol* **67**, 133–42 (1998).
7. Philipp-Staheli, J., Payne, S. R. & Kemp, C. J. p27(Kip1): regulation and function of a haploinsufficient tumor suppressor and its misregulation in cancer. *Exp Cell Res* **264**, 148–68 (2001).
8. Zhang, W. *et al.* A NIK-IKKalpha module expands ErbB2-induced tumor-initiating cells by stimulating nuclear export of p27/Kip1. *Cancer Cell* **23**, 647–59 (2013).
9. Chakkalakal, J. V. *et al.* Early forming label-retaining muscle stem cells require p27kip1 for maintenance of the primitive state. *Development* **141**, 1649–59 (2014).
10. Fero, M. L. *et al.* A syndrome of multiorgan hyperplasia with features of gigantism, tumorigenesis, and female sterility in p27(Kip1)-deficient mice. *Cell* **85**, 733–44 (1996).
11. Fero, M. L., Randel, E., Gurley, K. E., Roberts, J. M. & Kemp, C. J. The murine gene p27Kip1 is haplo-insufficient for tumour suppression. *Nature* **396**, 177–80 (1998).
12. Koh, K. N. *et al.* Persistent and heterogenous expression of the cyclin-dependent kinase inhibitor, p27KIP1, in rat hearts during development. *J Mol Cell Cardiol* **30**, 463–74 (1998).
13. Di Stefano, V., Giacca, M., Capogrossi, M. C., Crescenzi, M. & Martelli, F. Knockdown of cyclin-dependent kinase inhibitors induces cardiomyocyte re-entry in the cell cycle. *J Biol Chem* **286**, 8644–54 (2011).
14. Lloyd-Jones, D. *et al.* Heart disease and stroke statistics--2009 update: a report from the American Heart Association Statistics Committee and Stroke Statistics Subcommittee. *Circulation* **119**, e21–181 (2009).
15. Bartunek, J., Vanderheyden, M., Hill, J. & Terzic, A. Cells as biologics for cardiac repair in ischaemic heart failure. *Heart* **96**, 792–800 (2010).
16. Schumacher, B., Pecher, P., von Specht, B. U. & Stegmann, T. Induction of neoangiogenesis in ischemic myocardium by human growth factors: first clinical results of a new treatment of coronary heart disease. *Circulation* **97**, 645–50 (1998).
17. Giordano, F. J. *et al.* Intracoronary gene transfer of fibroblast growth factor-5 increases blood flow and contractile function in an ischemic region of the heart. *Nat Med* **2**, 534–9 (1996).
18. Harada, K. *et al.* Basic fibroblast growth factor improves myocardial function in chronically ischemic porcine hearts. *J Clin Invest* **94**, 623–30 (1994).
19. Pearlman, J. D. *et al.* Magnetic resonance mapping demonstrates benefits of VEGF-induced myocardial angiogenesis. *Nat Med* **1**, 1085–9 (1995).
20. Losordo, D. W. *et al.* Gene therapy for myocardial angiogenesis: initial clinical results with direct myocardial injection of phVEGF165 as sole therapy for myocardial ischemia. *Circulation* **98**, 2800–4 (1998).
21. Tao, Z. *et al.* Coexpression of VEGF and angiopoietin-1 promotes angiogenesis and cardiomyocyte proliferation reduces apoptosis in porcine myocardial infarction (MI) heart. *Proc Natl Acad Sci U S A* **108**, 2064–9 (2011).
22. Shyu, K. G., Manor, O., Magner, M., Yancopoulos, G. D. & Isner, J. M. Direct intramuscular injection of plasmid DNA encoding angiopoietin-1 but not angiopoietin-2 augments revascularization in the rabbit ischemic hindlimb. *Circulation* **98**, 2081–7 (1998).
23. Tao, Z. *et al.* HGF percutaneous endocardial injection induces cardiomyocyte proliferation and rescues cardiac function in pigs. *J Biomed Res* **24**, 198–206 (2010).
24. Han, J., Tsukada, Y., Hara, E., Kitamura, N. & Tanaka, T. Hepatocyte growth factor induces redistribution of p21(CIP1) and p27(KIP1) through ERK-dependent p16(INK4a) up-regulation, leading to cell cycle arrest at G1 in HepG2 hepatoma cells. *J Biol Chem* **280**, 31548–56 (2005).
25. Chandrasekher, G., Pothula, S., Maharaj, G. & Bazan, H. E. Differential effects of hepatocyte growth factor and keratinocyte growth factor on corneal epithelial cell cycle protein expression, cell survival, and growth. *Mol Vis* **20**, 24–37 (2014).
26. Watanabe, Y., Lee, S. W., Detmar, M., Ajioka, I. & Dvorak, H. F. Vascular permeability factor/vascular endothelial growth factor (VPF/VEGF) delays and induces escape from senescence in human dermal microvascular endothelial cells. *Oncogene* **14**, 2025–32 (1997).
27. Yu, L., Quinn, D. A., Garg, H. G. & Hales, C. A. Cyclin-dependent kinase inhibitor p27Kip1, but not p21WAF1/Cip1, is required for inhibition of hypoxia-induced pulmonary hypertension and remodeling by heparin in mice. *Circ Res* **97**, 937–45 (2005).
28. Guo, W. *et al.* IKK-beta/NF-kappaB p65 mediates p27 protein degradation in arsenite response. *Biochem Biophys Res Commun* (2014).
29. Prasad, R. C. *et al.* Identification of genes, including the gene encoding p27Kip1, regulated by serine 276 phosphorylation of the p65 subunit of NF-kappaB. *Cancer Lett* **275**, 139–49 (2009).
30. Hoefer, J. *et al.* Sphingosine-1-phosphate-dependent activation of p38 MAPK maintains elevated peripheral resistance in heart failure through increased myogenic vasoconstriction. *Circ Res* **107**, 923–33 (2010).
31. Fukuda, S. *et al.* Angiogenic signal triggered by ischemic stress induces myocardial repair in rat during chronic infarction. *J Mol Cell Cardiol* **36**, 547–59 (2004).
32. Pasumarthi, K. B. & Field, L. J. Cardiomyocyte cell cycle regulation. *Circ Res* **90**, 1044–54 (2002).

33. Poolman, R. A., Li, J. M., Durand, B. & Brooks, G. Altered expression of cell cycle proteins and prolonged duration of cardiac myocyte hyperplasia in p27KIP1 knockout mice. *Circ Res* **85**, 117–27 (1999).
34. Diez-Juan, A. & Andres, V. The growth suppressor p27(Kip1) protects against diet-induced atherosclerosis. *FASEB J* **15**, 1989–95 (2001).
35. Bussolino, F. *et al.* Hepatocyte growth factor is a potent angiogenic factor which stimulates endothelial cell motility and growth. *J Cell Biol* **119**, 629–41 (1992).
36. Rosen, E. M. *et al.* HGF/SF in angiogenesis. *Ciba Found Symp* **212**, 215–26; discussion 227–9 (1997).
37. Ferrara, N. Role of vascular endothelial growth factor in the regulation of angiogenesis. *Kidney Int* **56**, 794–814 (1999).
38. Lavu, M., Gundewar, S. & Lefer, D. J. Gene therapy for ischemic heart disease. *J Mol Cell Cardiol* **50**, 742–50 (2011).
39. Kiyokawa, H. *et al.* Enhanced growth of mice lacking the cyclin-dependent kinase inhibitor function of p27(Kip1). *Cell* **85**, 721–32 (1996).
40. Nakayama, K. *et al.* Mice lacking p27(Kip1) display increased body size, multiple organ hyperplasia, retinal dysplasia, and pituitary tumors. *Cell* **85**, 707–20 (1996).
41. Mathison, M. *et al.* In vivo cardiac cellular reprogramming efficacy is enhanced by angiogenic preconditioning of the infarcted myocardium with vascular endothelial growth factor. *J Am Heart Assoc* **1**, e005652 (2012).
42. Wu, F. Y. *et al.* Reduction of cytosolic p27(Kip1) inhibits cancer cell motility, survival, and tumorigenicity. *Cancer Res* **66**, 2162–72 (2006).
43. Kurrelmeyer, K. M. *et al.* Endogenous tumor necrosis factor protects the adult cardiac myocyte against ischemic-induced apoptosis in a murine model of acute myocardial infarction. *Proc Natl Acad Sci U S A* **97**, 5456–61 (2000).
44. Beg, A. A. & Baltimore, D. An essential role for NF-kappaB in preventing TNF-alpha-induced cell death. *Science* **274**, 782–4 (1996).
45. Abbott, A. Doubts over heart stem-cell therapy. *Nature* **509**, 15–6 (2014).

Acknowledgments

This work was granted financial support from the project supported by the National Natural Science Foundation of China (No. 81170102/H0203), the Priority Academic Program Development of Jiangsu Higher Education Institutions (BL2012011), the Chinese Medical Association of the Sunlight Foundation (SCRFCMDA201217), and the Fourth Period Progect "333" of Jiangsu Province (BRA2012207), China, Supporting program of Science and Technology of Jiangsu (Social Development, BK2010021).

Author contributions

N.Z., Y.Z. and Y.G. wrote the main manuscript text; N.Z., Y.F., Y.W., Y.G., H.M., P.C. and S.G. prepared figure 1/2; N.Z., Y.F., Y.G., Y.W. and M.Z. prepared figure 3/4; N.Z., Y.G. and Y.F. prepared figure 5/6; All authors reviewed the paper.

Additional information

Supplementary information accompanies this paper at http://www.nature.com/scientificreports

Competing financial interests: The authors declare no competing financial interests.

How to cite this article: Zhou, N. *et al.* p27^{kip1} haplo-insufficiency improves cardiac function in early-stages of myocardial infarction by protecting myocardium and increasing angiogenesis by promoting IKK activation. *Sci. Rep.* **4**, 5978; DOI:10.1038/srep05978 (2014).